Properties of SiC-Reinforced Aluminum Alloy Coatings Produced by the Cold Spray Deposition Process

E. Sansoucy, L. Ajdelsztajn, B. Jodoin
Department of Mechanical Engineering, University of Ottawa, Ottawa, Ontario, Canada

P. Marcoux
Vac Aero International Inc., Boucherville, Québec, Canada

Abstract

SiC-reinforced Al-12Si alloy coatings were produced using the Cold Gas Dynamic Spraying deposition process. Feedstock powder mixtures containing 20% and 30% of particulate SiC were used. The composite coatings' bond strengths and microstructures were evaluated, as well as the porosity and the SiC content. It was found that approximately 45% of the SiC particulate blended with the aluminum alloy was embedded in the coatings. The SiC was homogeneously distributed inside the Al-12Si matrix. Particle velocity measurements revealed that the addition of up to 30% vol. of SiC did not change the Al-12Si particle velocities.

Introduction

Metal matrix composites (MMCs) constitute a class of materials that continues to make major industrial impacts in fields as diverse as aerospace, automotives, and electronics. These materials can be tailored to yield superior properties by incorporating a controlled amount of reinforcements within a metal matrix. Alloys reinforced with ceramic particulates can offer property enhancements such as increased hardness, improved wear resistance, better thermal stability, and superior yield strength. Among the various matrix materials available, aluminum and its alloys are widely used in the fabrication of MMCs.

The addition of relatively inexpensive silicon carbide (SiC) particles to an aluminum alloy matrix has resulted in an increased strength [1], elastic modulus [1], and wear resistance [2], while providing good corrosion resistance. These composites have emerged as an important class of high-performance structural elements in the automotive and space industries [3, 4]. Major fabrication methods of these aluminum SiC composites include casting, extrusion, thermal spray deposition, and powder metallurgy [5]. Defects such as porosity, shrinkage, oxide inclusions, clustering of silicon carbide particles, and degradation of the reinforcement significantly influence the composite properties [1, 5]. For example, low-temperature ductility and poor toughness are drawbacks that limit the performance and applications of such composites. Al-SiC composite coatings produced by plasma spraying have yielded properties that are characteristic of bulk composites [6]. As a result, these coatings are a viable method to improve the surface properties without producing any significant change in the ductility of the components [7].

The SiC particle distribution and volume fraction in plasma sprayed composite coatings depend on the quality of the feedstock powder being used during spraying. In feedstock powders prepared by blending SiC with aluminum alloy particles, SiC particles are preferentially lost compared to the aluminum alloy particles [8]. Excess SiC must then be added to the feedstock to compensate for the SiC lost during the spraying process. When the SiC level in the feedstock exceeds a certain value, further addition of the SiC particles in the feedstock no longer increases the SiC volume fraction in the coating. The large difference in melting temperatures between the SiC and the aluminum alloy, and poor wettability of SiC by the aluminum explain this behavior [8]. Uniformly distributed reinforcements within an aluminum alloy matrix, especially when the reinforcements exceed 30% volume, can be obtained through mechanical alloying.

The Cold Gas Dynamic Spraying (CGDS) process is an emerging thermal spray coating technology that can produce conventional [9-11], nanocrystalline [12-14], and amorphous coatings [15, 16]. In this process, the powder particles are neither in a softened, semi-molten, nor molten state but remain in their solid state throughout the deposition process. Fine powder particles are injected in a supersonic gas flow and accelerated above a critical velocity. Upon impact on the substrate, the particles deform plastically and bond to the substrate to form a coating [10, 17]. The process is also capable of depositing a wide variety of aluminum alloy [18-20] and composite coatings [18, 21-24].

Few studies have looked at the mechanical properties of aluminum alloy coatings reinforced with SiC particulates produced by the CGDS process although it has been shown that deposits of hard materials such as SiC and Al_2O_3 incorporated in a ductile aluminum matrix can be successfully produced by the CGDS process [23]. The thickness of the Al-SiC composite films could reach 50 µm when spraying on silicone substrates. It has also been shown that changing the content of SiC particulates within an aluminum matrix produces predictable changes in thermal properties such as the thermal conductivity and the coefficient of thermal expansion [21]. Composite coatings using an aluminum matrix with reinforcing particles of diamond, tungsten, silicon carbide, or aluminum nitride have also been produced using the CGDS process [22].

The objectives of this study are to develop and evaluate the properties of Al-12Si alloy coatings reinforced with dispersed SiC particles using the CGDS process. This paper examines the effects of the ceramic particulate content of the feedstock powder on the coatings' mechanical properties and microstructure.

Experimental Procedures

Powder Preparation

The materials used in this study comprised of aluminum Al-12Si powder (Praxair Al-111) and a reinforcement phase of particulate SiC. The aluminum alloy was composed of particles ranging between 5 to 45 µm in diameter. As shown in Fig. 1a, these particles have a spherical morphology. The morphology of the SiC particles is angular (Fig. 1b). Even though the SiC particles are slightly denser than the Al-12Si particles, both are expected to reach similar velocities as irregular shaped particles have been shown to experience larger drag coefficients than spherical particles [25]. The reinforcement particles were sieved below 25 µm using a 500-mesh sieve and mixed to the matrix alloy powder to create a blend powder containing 20% volume of SiC. A mixture with 30% volume of SiC was produced from SiC particles sieved below 32 µm using a 400-mesh sieve. A description of the mixtures is presented in Table 1.

Coating Preparation

The SiC-reinforced aluminum alloy coatings were produced using the CGDS coating system developed at the University of Ottawa Cold Spray Laboratory. The system includes a spray chamber, a spray gun, a propellant gas heater, and a commercial powder feeder (Praxair Surface Technologies model 1264, Concord, NH, USA). The spray gun consists of a converging-diverging nozzle with an exit diameter of 7.3 mm. For the present work, helium was used as propellant gas. The gas stagnation pressure and its stagnation temperature were set at 1.7 MPa and 360°C, respectively. The coatings were produced on grit-blasted 6061-T6 aluminum substrates at a stand-off distance of 10 mm. The substrates were grit blasted using ebony (ferrosilicate) beads (20-grit) at blasting pressure of 400 kPa (60 psi) and at a 45° blasting angle.

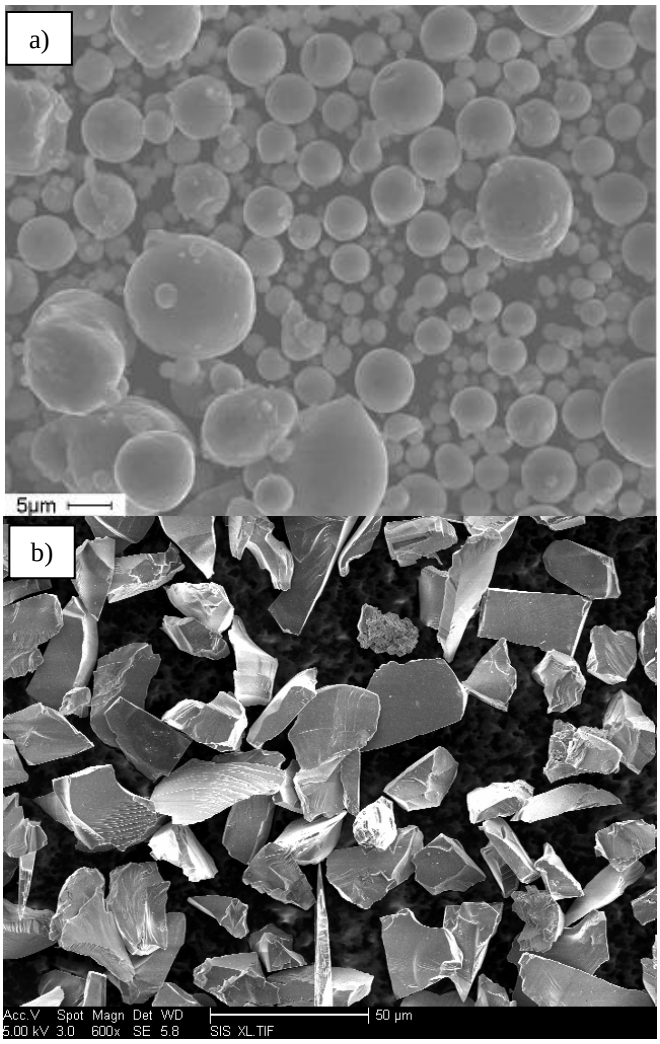

Figure 1: Morphology of a) the Al-12Si and b) the SiC powders.

Table 1: Description of the composite powders.

Composite powders	SiC (% vol.)	SiC size (µm)
Al-12Si + 30% SiC	30	< 32
Al-12Si + 20% SiC	20	< 25

Coating Characterization

The coatings samples were sectioned, and prepared for scanning electron microscopy (SEM), following standard metallographic techniques. Secondary electron and backscattered electron images of the coatings' cross-sections were used to evaluate the microstructural features such as the porosity and the volume fraction of the SiC. These were obtained using a public domain software, imageJ [26]. A

quantitative separation of the coating's structural elements was performed based on the grey level distribution of the SEM images. The porosity (black contrast) and the SiC particles (deep grey contrast) could be distinguished by setting grey scale threshold cutoff points. The percent areas of the marked regions for porosity and for the SiC particles could then be measured separately.

Bond strength evaluations were conducted using the ASTM Standard C 633-01 [27]. Coatings were produced on grit-blasted standard test samples having a 25.4 mm diameter and an overall length of 38.1 mm. Several passes were carried out, with a 50% pass overlap, to cover the entire surface of the sample. The top portion of the coating was then machined flat and glued to an uncoated test sample using an adhesive (Master Bond EP-15, Hackensack, NJ, USA). The assembled parts were then cured at 170°C for 90 minutes in a V block device that ensures proper alignment. Before testing the coatings, the bonding agent was tested separately on four uncoated test samples, and failed at 82 ± 10 MPa, which conforms to the product specifications.

Particle Velocity Measurements

Particle velocities were measured using the DPV-CPS (Tecnar Automation Ltd., St-Bruno, Québec, Canada), a laser in-flight diagnostic system. While a continuous laser illuminates a measurement volume, a dual-slit photomask captures the signal generated by individual particles passing in front of the sensor. The signal from the photosensor is then amplified, filtered, and analyzed. In-flight diagnostic of each individual particle that crosses the measurement volume is performed by determining the time between the two peaks of the particle signal. The particle velocities are then obtained by dividing the distance between the two slits by the particle's flight time [28]. In this study, the velocity measurements were taken at a location 5 mm from the spray gun exit. In order to avoid particle build-ups and rebounds that could obstruct the sensor field of view, the particle velocity measurements were performed without the presence of a substrate at the exit of the spray gun.

Results and Discussion

Coatings' Microstructures

The SEM images of the cross-section of CGDS coatings using the Al-12Si and Al-12Si+30% SiC powders are presented in Figs. 2 and 3, respectively. The coatings synthesized from the Al-12Si+20% SiC exhibited a similar overall microstructure. These coatings were obtained from a single pass of the spray gun over the substrates. The entire coating and a close-up of the substrate-coating interface are presented. The measured thickness, porosity, and SiC content in the coatings obtained from the SEM images analysis are summarized in Table 2. The coating thickness, approximately 1200 µm, was not influenced by the addition of SiC particles with the Al-12Si powder.

The interface of the Al-12Si coating (Fig. 2a) contains some pores and small cracks at the substrate-coating interface. It is believed that these defects occurred during the metallographic preparation of the sample. The coatings reinforced with 30% vol. SiC particles (Fig. 3a) display an interface free of cracks or pores. In the composite coatings, the particulate reinforcements are randomly distributed but homogeneously dispersed inside the aluminum alloy matrix, as illustrated in Figs. 4 and 5. The coatings consist of deformed Al-12Si particles that surround SiC particles. At impact, the SiC particles did not deform but became confined by the Al-12Si. These ductile particles subsequently deformed around the hard SiC.

The addition of SiC particles to the Al-12Si powder increases the porosity of the resulting composite coatings. The compaction of the previously deposited layers of material by impinging particles may be reduced due to the presence of SiC embedded in the coating. During the deposition process, the SiC particles did not plastically deform and the voids around the reinforcement phase of the coating remained unfilled. The analysis demonstrated that the coatings became more porous when the SiC content of the feedstock powder was increased from 20 to 30 volume percent. The additional impinging SiC particles on the coating do not lower the porosity but create more voids as they become embedded in the coating.

Table 2: Properties of the coatings microstructure.

Coatings	Thickness (µm)	Porosity (%)	SiC (vol. %)
Al-12Si	1200	0.1	N/A
Al-12Si + 20% SiC	1200	0.8	9
Al-12Si + 30% SiC	1200	1.3	14

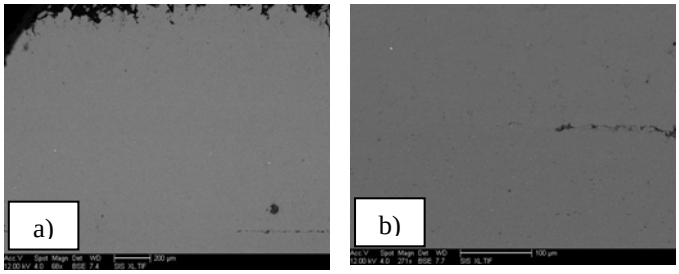

Figure 2: SEM images of the cross-section of an Al-12Si coating showing a) the entire coating and b) the substrate-coating interface.

In the current study, approximately 45% of the SiC volume fraction was found in the coatings. This is slightly higher than what was found in another study, where 40% of the SiC was retained in the coatings [21].

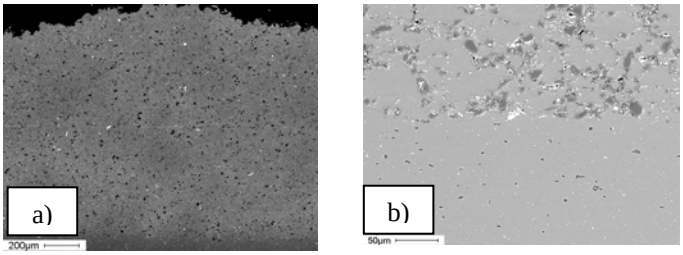

Figure 3: SEM images of the cross-section of an Al-12Si coating reinforced with 30% vol. SiC particles below 32 µm showing a) the entire coating and b) the substrate-coating interface.

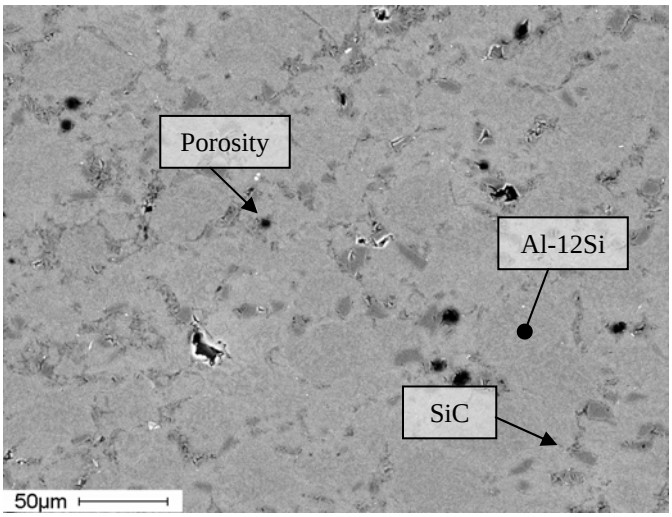

Figure 4: SEM image of the cross-section of an Al-12Si coating reinforced with 20% vol. SiC particles below 25 µm. The grey regions and the darker spots correspond to the Al-12Si and the SiC, respectively.

Bond Strength

Adhesion strength of 49 MPa was obtained during the bond strength test for the Al-12Si coating. Examination of the specimens revealed that the failure occurred at the coating-substrate interface. Most of the coating remained attached to the specimen on which the bonding agent was applied, as shown in Fig. 6.

Bond strengths values 44 and 43 MPa were obtained for Al-12Si+20% SiC and Al-12Si+30% SiC coatings, respectively. These values correspond to adhesion strengths since the arrangements also failed at the substrate-coating interface. The inclusion of SiC particles did not appreciably influence the degree of adhesion of the coatings on the substrates. The SEM images of the SiC-reinforced coatings revealed substrate-coating interfaces free of defects that could alter the adherence of the coating.

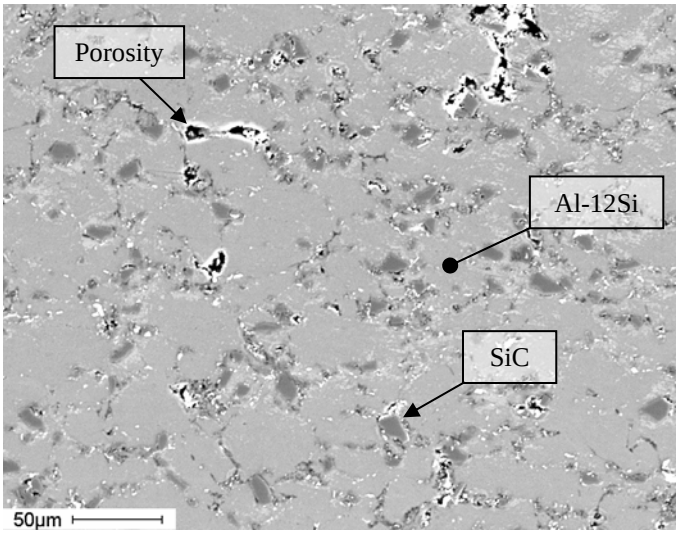

Figure 5: SEM image of the cross-section of an Al-12Si coating reinforced with 30% vol. SiC particles below 32 µm. The grey regions and the darker spots correspond to the Al-12Si and the SiC, respectively.

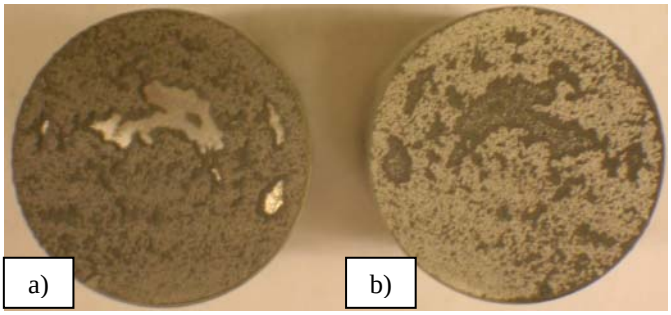

Figure 6: Photograph of the bond strength specimens with a) the bonding agent and b) the remainder of the Al-12Si coating after the bond test.

Particle Velocity

Figure 7 presents the measured particle velocity distribution for the Al-12Si under the spraying conditions stated above. The particle velocities range between 350 and 900 m/s, with an average of 559 ± 132 m/s. Under the same spraying conditions, the measured particle velocity distribution for the Al-12Si+30% SiC is showed in Fig. 8. The particle velocities are situated between 350 m/s and 900 m/s as well, with an average of 581 ± 115 m/s. Adding 30% vol. of SiC particles below 32 µm did not produce a significant change on the particle velocities. The variations in the coating properties were not as a result of different particle velocities but due to the presence of SiC particles in the feedstock powder.

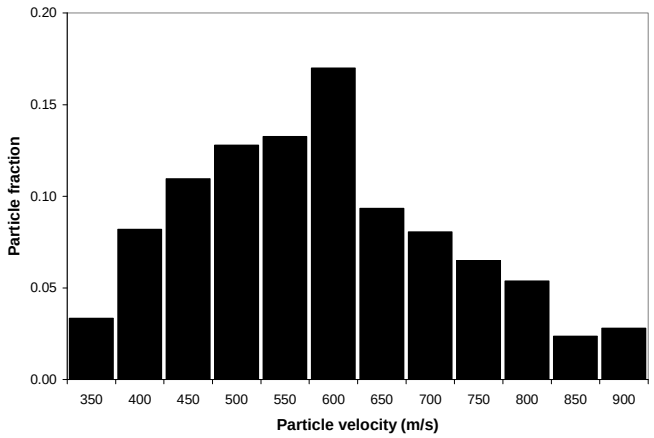

Figure 7: Measured particle velocity distribution of the Al-12Si powder.

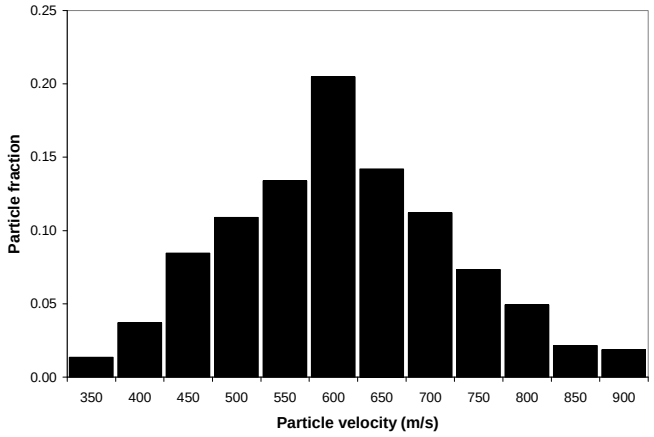

Figure 8: Measured particle velocity distribution of the Al-12Si powder with 30% vol. of SiC particles below 32 µm.

Conclusions

SiC-reinforced aluminum alloy coatings were successfully produced by the CGDS process. The composite coatings microstructure, thickness, porosity, and composition were compared to an Al-12Si coating. The results show that 45% of the SiC mixed with the aluminum matrix was retained in the composite coatings. These SiC particles exhibit a reasonably uniform distribution within the aluminum matrix. The coating thickness and adhesion strength were not affected by the SiC content. However, the coatings became more porous by increasing the SiC volume content of the blended powders.

Acknowledgements

The authors wish to acknowledge the financial support of Natural Sciences and Engineering Research Council of Canada (NSERC) as well as the Centre québécois de recherche et de développement de l'aluminium (CQRDA). They also thank Dr. Mathieu Brochu of McGill University for his help with the SEM samples preparation and characterization. The assistance of Chrystelle Thibault Boyer with the powder preparation and with the coating production is appreciated.

.

References

1. Ü. Cöcen, and K. Önel, Ductility and strength of extruded SiC_p/aluminum-alloy composites, *Compos. Sci. Technol.*, Vol 62, 2002, p 275-282
2. S.C. Tjong, S.Q. Wu, and H.C. Liao, Wear Behavior of an Al-12% Si Alloy Reinforced With a low Volume Fraction of SiC Particles, *Compos. Sci. Technol.*, Vol 57, 1997, p 1551-1558
3. T.F. Klimowicz, The Large-Scale Commercialization of Aluminum-Matrix Composites, *J. Metals*, Vol 46 (No. 11), 1994, p 49-53
4. D.M. Schuster, M.D. Skibo, R.S Bruski, R. Provencher, and G. Riverin, The Recycling and Reclamation of Metal-Matrix Composites, *J. Metals*, Vol 45 (No. 5), 1993, p 26-30
5. T.P.D. Rajan, R.M. Pillai, and B.C. Pai, Review: Reinforcement coatings and interfaces in aluminum metal matrix composites, *J. Mater. Sci.*, Vol 33, 1998, p 3491-3503
6. R. Tiwari, H. Herman, S. Sampath, and B. Gudmundsson, Plasma spray consolidation of high temperature composites, *Mater. Sci. Eng.*, Vol A144, 1991, p 127-131
7. K. Ghosh, T. Troczynski, and A.C.D. Chaklader, Aluminum-Silicone Carbide Coatings by Plasma Spraying, *J. Therm. Spray Technol.*, Vol 7 (No. 1), 1998, p 78-86
8. M. Gui, S.B. Kang, and K. Euh, Al-SiC Powder Preparation for Electronic Packaging Aluminum Composites by Plasma Spray Processing, *J. Therm. Spray Technol.*, Vol 13 (No. 2), 2004, p 214-222
9. A.P. Alkhimov, V.F. Kosarev, and A.N. Papyrin, A method of cold gas-dynamic deposition, *Sov. Phys. Dokl.*, Vol 35, 1990, p 1047-1049
10. A.P. Alkhimov, A.N. Papyrin, and V.F. Kosarev, US Patent 5 302 414, 1994
11. T.H. Van Steenkiste, and J.R. Smith, Evaluation of Coatings Produced Via Kinetic and Cold Spray Processes, *J. Therm. Spray Technol.*, Vol 13 (No. 2), 2004, p 274-282
12. V. Shukla, G.S. Elliot, and B.H. Kear, Nanopowder Deposition by Supersonic Rectangular Jet Impingement, *J. Therm. Spray Technol.*, Vol 9 (No. 3), 2000, p 394-398
13. R.S. Lima, J. Karthikeyan, C.M. Kay, J. Lindermann, and C.C. Berndt, Microstructural characteristics of cold-sprayed nanostructured WC-Co coatings, *Thin Solid Films*, Vol 416, 2002, p 129-135
14. L. Ajdelsztajn, B. Jodoin, G.E. Kim, and J.M. Schoenung, and J. Mondoux, Cold Spray Deposition of Nanocrystalline Aluminum Alloys, *Metall. Mater. Trans. A*, Vol 36, 2005, p 657-666

15. L. Ajdelsztajn, E.J. Lavernia, B. Jodoin, P. Richer, and E. Sansoucy, Cold Gas Dynamic Spraying of Fe-based Amorphous Alloy, *Building on 100 Years of Success: Proceedings of the 2006 International Thermal Spray Conference*, B.R. Marple, M.M. Hyland, Y.C. Lau, R.S. Lima, and J. Voyer, Eds., May 15-18, 2006 (Seattle, WA, USA), ASM International, 2006
16. S. Yoon, H.J. Kim, and C. Lee, Deposition behavior of bulk amorphous NiTiZrSiSn according to the kinetic and thermal energy levels in the kinetic spraying process, *Surf. Coat. Technol.*, Vol 200, 2006, p 6022-6029
17. R.C. Dykhuizen, and M.F. Smith, Gas Dynamics Principles of Cold Spray, *J. Therm. Spray Technol.*, Vol 7 (No. 2), 1998, p 205-212
18. E. Sansoucy, B. Jodoin, P. Richer, and L. Ajdelsztajn, Effect of Spraying Parameters on the Microstructure and Bond Strength of Cold Spray Aluminum Alloy Coatings, *Building on 100 Years of Success: Proceedings of the 2006 International Thermal Spray Conference*, B.R. Marple, M.M. Hyland, Y.C. Lau, R.S. Lima, and J. Voyer, Eds., May 15-18, 2006 (Seattle, WA, USA), ASM International, 2006
19. L. Ajdelsztajn, A. Zúñiga, B. Jodoin, and E.J. Lavernia, Cold-Spray Processing of a Nanocrystalline Al-Cu-Mg-Fe-Ni Alloy with Sc, *J. Therm. Spray Technol.*, Vol 15 (No. 2), 2006, p 184-190
20. L. Zhao, K. Bobzin, D. He, J. Zwick, F. Ernst, and E. Lugscheider, Deposition of Aluminum Alloy Al12Si by Cold Spraying, *Adv. Eng. Mater.*, Vol 8 (No. 4), 2006, p 264-267
21. G.L. Eesly, A. Elmoursi, and N. Patel, Thermal properties of kinetic spray Al-SiC metal-matrix composite, *J. Mater. Res.*, Vol 18 (No. 4), 2003, p 855-860
22. T.H. Van Steenkiste, A. Elmoursi, D. Gorkiewicz, and B. Gillispie, Fracture study of aluminum composite coatings produced by the kinetic spray method, *Surf. Coat. Technol.*, Vol 194, 2005, p 103-110
23. H.Y. Lee, Y.H. Yu, Y.C. Lee, Y.P. Hong, and K.H. Ko, Cold Spray of SiC and Al_2O_3 With Soft Metal Incorporation: A Technical Contribution, *J. Therm. Spray Technol.*, Vol 13 (No. 2), 2004, p 184-189
24. Z.B. Zhao, B.A. Gillispie, and J.R. Smith, Coating deposition by the kinetic spray process, *Surf. Coat. Technol.*, Vol 200, 2006, p 4746-4754
25. B. Jodoin, L. Ajdelsztajn, E. Sansoucy, A. Zúñiga, P. Richer, and E.J. Lavernia, Effect of particle size, morphology, and hardness on cold gas dynamic sprayed aluminum alloy coatings, *Surf. Coat. Technol.*, In Press, Corrected Proof, Available online 15 September 2006
26. W. Rasband, National Institute of Health, USA, http://rsb.info.nih.gov/ij/
27. ASTM C 633-01, "Standard Test Method for Adhesion or Cohesion Strength of Thermal Spray Coatings," *Annual Book of ASTM Standards*, Vol. 02.05, ASTM
28. DPV-2000 – Reference Manual Rev. 5.0, Tecnar Automation, 45 pages